ANALYSIS OF EUTECTIC AND METALLIC MELT FLOW AND BLOCKAGE IN BWR CONTROL ROD GUIDE TUBE BY MPS METHOD

YUTO GOTO*, AKIFUMI YAMAJI

Cooperative Major in Nuclear Energy, Graduate School of Advanced Science and Engineering, Faculty of Science and Engineering, Waseda University

3-4-1 Okubo, Shinjuku-ku, Tokyo 169-8555, Japan

ABSTRACT

Moving Particle Semi-implicit (MPS) method has been applied to analyze melt behavior through a control rod guide tube and investigate possible conditions for formation of blockages by metallic Zr and SS-B_4C eutectic melt during postulated dry core degradation in severe accident of a boiling water reactor (BWR). The preliminary analysis results show that blockage would form from the side of the control rod and above the velocity limiter. The analysis results also show that formation of the blockage depends on inflow mass rate, initial temperature of the melt, and the melt properties such as solidus temperature and latent heat. However, the melt inflow boundary condition may have to be revised to simulate the accident condition. Moreover, further development of the MPS method may be necessary to simulate fast heat transfer between the melt and the control rod guide tube.

1. Introduction

In the combined effort for decommissioning of the damaged reactors unit 1, 2 and 3 in Fukushima Daiichi Nuclear Power Plant (NPP), the necessity to improve understanding of the core degradation process in a boiling water reactor (BWR) has become evident [1]. However, it has been revealed that different analysis codes and analysists predict different core degradation scenarios for the Fukushima reactors [2]. Moreover, it has become evident that even with a set of well-defined boundary conditions, predictions with different analysis codes begin to diverge after onset of core degradations [3]. Consequently, a molten pool formation is predicted by MAAP5 in the core region of the Fukushima unit 1, but such molten pool formation is not predicted by MELCOR2.1 [3].

It is suggested that part of the reasons for the above mentioned difference, among numerous other reasons, is due to the difference in modeling gas (mainly steam) flow blockage [3]. In early phase of a BWR core degradation, some metals such as stainless steel (SS) and zirconium (Zr) are expected to melt at relatively low temperature (1400–2100(K)), before degradation of the oxide fuels begin, depending on the eutectic formation (e.g.,

SS-B_4C eutectic of the BWR control rod) and oxidation state of the metals (e.g., metallic Zr) [4]. In the Fukushima Daiichi NPP accidents, the melt relocation was considered to occur mainly after the water level decreased below the bottom of the active fuel [5]. Under such dry core conditions, steam generation was considered to be insufficient to make a dense crust and the molten metals were considered to fall through some continuous drainage paths at the lower core support plate, around the fuel support pieces, such as control rod guide tubes and instrumentation tubes [5].

However, limited experimental evidence, such as XR-2 experiment [6] and CORA-33 experiment [7], indicates that although most of the metals are likely to have flown through the fuel channels and the core support plate at the end of the process, there may be partial and / or temporal blockage formed during such dry core degradation process [6]. However, it is difficult to deduce the exact conditions and materials, which formed such blockages from these experiments. Most severe accident analysis codes are also limited in capabilities to predict such melt flow through / blockage conditions (e.g., melt temperature and flow rate), because these codes adopt lumped parameter methods and often rely on numerous parameter adjustments from limited validations with experiments [8, 9]. Hence, more mechanistic method, which is capable of simulating evolution of solid-liquid phase interface, is necessary to identify the melt flow through / blockage conditions and mechanisms.

Moving Particle Semi-implicit (MPS) method is one of the particle methods for incompressible flow. As a Lagrangian method, MPS method discretizes the computation domain with calculation points (expressed as “particles”) instead of meshes. As the result, MPS method can easily and accurately capture free surface, interface and fluid thermo-physical properties without relying on empirical correlations [10]. The MPS method has been extensively studied and developed for simulations of degraded fuel behavior in a severe accident. For example, one of the preceding studies addressed the EPRI-3 test, which involved freezing behavior of molten Al_2O_3 in the full length Westinghouse PWR instrument tube as it flowed down the tube and solidified [11]. The MPS simulation well-predicted the heat transfer from the melt to the instrument tube and the penetration length, which demonstrated the capability of the developed MPS method to accurately model melt flows involving heat transfer and solidifications in tubes [12].

Hence, the objectives of this study are to analyze metallic Zr and SS-B_4C eutectic melt behaviors through a control rod guide tube of BWR by MPS method and to clarify pathway blockage mechanism and conditions (melt initial temperature and flow rate). As was simulated in the XR-2 experiment, in the early phase of dry core degradation, SS-B_4C eutectic melting of the control rod is expected to occur at 1420(K), followed by melting of Zr at 2098(K) [12]. These melts are expected to flow through the control rod guide tube.

2. Numerical method and models

2.1 MPS method

The governing equations in MPS method are mass, momentum and energy conservation as shown in Eqs. (1), (2), and (3), respectively [10]:

$$\frac{D\rho}{Dt} = 0 \tag{1}$$

$$\frac{D\boldsymbol{u}}{Dt} = -\frac{1}{\rho}\nabla P + \nu\nabla^2\boldsymbol{u} + \boldsymbol{g} + \boldsymbol{f} \tag{2}$$

$$\frac{Dh}{Dt} = k\nabla^2 T + Q \tag{3}$$

where ρ is density, $\boldsymbol{u}$ is velocity vector, P is pressure, ν is kinematic viscosity, $\boldsymbol{g}$ is gravity, $\boldsymbol{f}$ is surface tension force, h is enthalpy, T is temperature, k is heat conductivity, and Q is heat source.

In MPS method, the differential operators in the governing equations are substituted according to particle interaction models such as gradient, divergence and Laplacian. These interaction models are applied for neighboring particles by the following weight function. The weight function is defined as:

$$w(r) = \begin{cases} \dfrac{r_e}{r} - 1 & (0 \le r \le r_e) \\ 0 & (r_e \le r) \end{cases} \tag{4}$$

where r is the distance between particles, r_e is the effective interaction radius that determines neighboring particles [10].

The particle number density of particle i at the position is r_i is sum of weight function:

$$n_i = \sum_{j \neq i} w\left(|\boldsymbol{r_j} - \boldsymbol{r_i}|\right) \tag{5}$$

MPS method is dedicated to imcompressible flow so that the particle number density is kept constant at the initial value n^0 during the calculation.

The gradient model and Laplacian models are used for discretizing differential operators in the governing equations. Gradient and Laplacian models are defined as follows, respectively:

$$\langle\nabla\Phi\rangle_i = \frac{d}{n^0}\sum_{j \neq i}\left[\frac{(\Phi_j - \Phi_i)(\boldsymbol{r_j} - \boldsymbol{r_i})}{|\boldsymbol{r_j} - \boldsymbol{r_i}|^2} w\left(|\boldsymbol{r_j} - \boldsymbol{r_i}|\right)\right] \tag{6}$$

$$\langle \nabla^2 \Phi \rangle_i = \frac{2d}{\lambda n^0} \sum_{j \neq i} \left[\left(\Phi_j - \Phi_i \right) w\left(|\boldsymbol{r_j} - \boldsymbol{r_i}| \right) \right] \tag{7}$$

where Φ is physical schalar quatity, d is the number of spatial dimensions, and λ is the coefficient of Laplacian model defined as:

$$\lambda = \frac{\sum_{j \neq i} |\boldsymbol{r_j} - \boldsymbol{r_i}|^2 w\left(|\boldsymbol{r_j} - \boldsymbol{r_i}| \right)}{\sum_{j \neq i} w\left(|\boldsymbol{r_j} - \boldsymbol{r_i}| \right)} \tag{8}$$

A semi-implicit algorithm is applied to MPS method by solving explicitly the gravity term and surface tension term, and implicitly the pressure term in the momentum equation. In addition, when highly viscous fluids are used, computational cost is saved due to avoiding use of small calculation time steps by implicitly solving the viscosity term [14].

2.2 Heat transfer, phase change, and viscosity models

When melt such as SS-B_4C and Zr flows through the control rod guide tube, intensive heat transfer from the melt to the guide tube is expected. By the heat transfer, some of the melt may solidify and form blockage in the channel depending on the different inflow and boundary conditions. Hence, the following models are incorporated in the current MPS simulation.

Enthalpy of particles is explicitly calculated by discretizing energy equation as follows:

$$h_i^{k+1} = h_i^k + k\Delta t \cdot \frac{2d}{n^0 \lambda} \sum_{j \neq i} \left(T_j^k - T_i^k \right) w_{ij} + Q \tag{9}$$

When heat transfer between two different materials is calculated, the thermal conductivity is expressed by a harmonic mean of the thermal conductivities of the two materials as follows:

$$k = \frac{2k_i k_j}{k_i + k_j} \tag{10}$$

where k_i and k_j are respectively thermal conductivities of particle i and particle j[14]. The above expression is derived from a simple assumption that heat flux from the particle into the midpoint of the two particles is equal to the heat flux from the midpoint to the other particle [15].

The radiation heat transfer is modeled as heat removal from free surface particles of melt and based on Stefan-Boltzman law. The radiated power Q is calculated as:

$$Q = A\varepsilon\sigma T^4 \tag{11}$$

Where, A is radiation surface area, ε is emissivity, σ is Stefan-Boltzman constant ($5.67 \times 10^{-8} W/(m^2 K^4)$), and ε is emissivity dependent on surface form and material property.

Melting and solidification processes need to be modeled for analysis of melt behavior through a control rod guide tube. As explained in Section 2.1, enthalpy of the fluid (particle) can be mechanistically calculated by discretizing energy conservation equation with the Laplacian model for differential operator in MPS. Hence, thermo-physical properties of the fluid can be tracked and determined mechanistically from the local fluid enthalpy. As the result, mechanistic modeling of phase change is possible. The relation between temperature and enthalpy for solid, liquid and phase transition stages are expressed as follows:

$$T = \begin{cases} T_s + \dfrac{h - h_{s0}}{\rho C_{ps}} & (h < h_{s0}) \\ T_s & (h_{s0} \le h \le h_{s1}) \\ T_s + \dfrac{h - h_{s1}}{\rho C_{pl}} & (h_{s1} < h) \end{cases} \tag{12}$$

where T_s is the solidus temperature, h_{s0} is the enthalpy at the end of solidification, h_{s1} is the enthalpy at the beginning of solidification, C_{ps} and C_{pl} are specific heat in solid and fluid state, respectively.

In the modeling of phase change, the concept of solid fraction γ is introduced to identify the state of a particle and is expressed as follows:

$$\gamma = \begin{cases} 1 & (h < h_{s0}) \\ \dfrac{h_{s1} - h}{h_{s1} - h_{s0}} & (h_{s0} \le h \le h_{s1}) \\ 0 & (h_{s1} < h) \end{cases} \tag{13}$$

When $\gamma = 1$, the particle is in completely solid state; when $\gamma = 0$, the particle is in completely fluid state. When $0 < \gamma < 1$, the particle is in partially fluid and partially solid state [16]. As was adopted in the preceding study, the followings are assumed in this study to model the melt solidification and channel blockage [12]. The status of a particle is judged as fluid when its solid fraction is below a threshold (0.55 and solid when it is greater than the threshold. The solidified particles are assumed to continue following the Navier-Stokes equation as fluid until it is in contact with the wall particle. At this contact, the particle is assumed to stick to the wall particle and is immobilized (i.e., its coordinate is fixed) [12]. Any solid particles in contact with the immobilized particle is also assumed to stick and thus form a crust layer, which may eventually block the channel unless it is remelted.

The viscosity of molten materials in a phase transition stage would have some influence on

analysis of melt flow in a control rod guide tube. The viscosity in a phase transition stage is often expressed as a function of solid fraction. In this study, the following model, proposed by Ramacciotti et al. [17], is used:

$$\nu = \nu_0 exp(2.5 \cdot C \cdot \gamma) \quad (14)$$

where ν_0 is the kinematic viscosity in a fluid state and C is the constant parameter depending on the material, which generally take the value between 4 and 8 for molten metal.

3. Simulation conditions

The BWR full-scale fuel support piece was simulated including the control rod guide tube, with particle size of 3(mm) as shown in **Fig 1.** for coarse resolution calculations. Furthermore, in order to reduce calculation cost, the quarter symmetric geometry is modeled with particle size of 1.5(mm) for fine resolution calculations. The dummy wall particles are used to define the quarter symmetric geometry for which pressure is calculated while heat calculation is excluded.

The inflow particles are used at the upper boundary, which generates new melt particles at the specified inflow rate and temperature. The adiabatic boundary is assumed at the outer surface of the fuel support piece while radiation boundary is defined for the free surface of the melt, which is defined by the surface with particle number density of less than $0.97n^0$.

Physical properties of the materials assumed in this study are listed on **Tab 1**. These physical properties were quoted from MELCOR reference manual [8]. $\mathrm{SS\text{-}B_4C}$ eutectic property is estimated from weighted average of SS and B_4C composing a control rod [17].

For simulation cases, the initial wall temperature is determined as 600(K) by referring to XR2 test [6]. The initial conditions for different simulation cases are listed in **Tab 2**. As described in Chapter 1, SS-B_4C and Z are considered as the incoming melts. For the full-scale fuel support piece geometry, the total inflow mass of SS-B_4C is determined as 78.3(kg) by assuming complete melting of one control rod [17], and that of Zr is determined by assuming complete melting of a channel box [18]. Case numbers with “C” and “F” denote simulations with coarse resolution (particle size of 3.0(mm)) and fine resolution (particle size of 1.5(mm)), respectively. The other parameters were provisionally decided due to limited experimental and reference data.

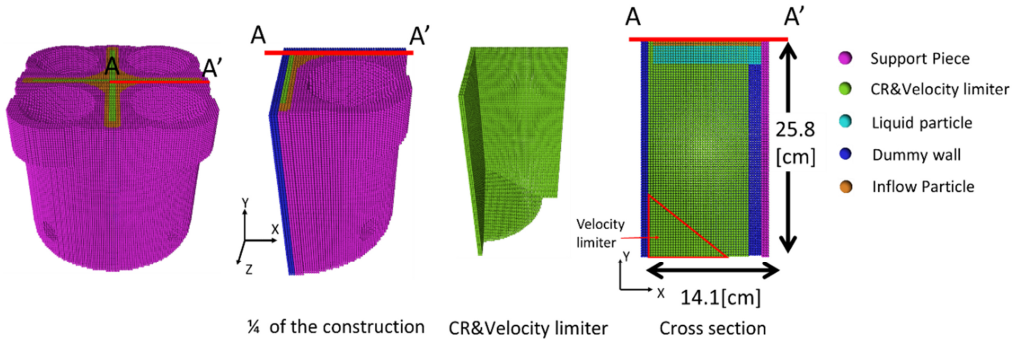

Fig1. Initial particle configuration for simulation.

Property	SS-B_4C	Zr	SS (wall particle)
Density (kg/m^3)	6645.5	6520.0	7930.0
Specific heat (J/kg*K)	451.8	376.6	840
Melting temperature (K)	1420	2098	1700
Heat conductivity (J/kg*K)	30.8	58.24	21.0
Latent heat (kJ/kg)	289	225	268

Tab 1: Physical property of the materials.

Case number	1C	1F	2C	2F	3C	3F	4C	4F*
Inflow melt	SS-B_4C		Zr					
Total inflow mass (kg)	78.3		47.75					
Inflow rate (kg/s)	5	←	5	←	25	←	5	←
Initial melt temperature (super heat) (K)	1450 (30)	←	2118 (20)	←	←	←	2318 (220)	←
Particle size (mm)	3.0	1.5	3.0	1.5	3.0	1.5	3.0	1.5

C: Coarse particle resolution F: Fine particle resolution

*Case4 F: currently being calculated

Tab 2: Initial conditions for different simulation cases.

4. Results and discussions

4.1 Simulations with SS-B_4C eutectic melt

Figure 2 shows a series of representative moments for cases 1C and 1F. In case 1C, a few particles were solidified and almost all particles were discharged from the bottom, but in case 1F, the channels by the side and edge of the control rod blade was completely blocked by about 5(s). In Case 1F, significant solidification was also simulated near the center of the configuration, which accumulated above the velocity limiter, but the blockage was not completed by the end of the simulation.

In fact, the case 1F simulation terminated at about 7(s) as the blockage built up and

reached the melt inflow boundary, where abnormal velocities were calculated by collisions of the inflow particle and the blockage. **Figure 3** shows discharged mass of the melt from the bottom of the fuel support piece for the two cases. After about 3(s), the discharged mass rate of case 1F is equal to that of case 1C despite formation of blockages. This is because the inflow boundary is fixed at 5(kg/s) and the inlet melt is forced to flow through the partially blocked channels. Hence, it may be necessary to consider other inflow boundary conditions, such as preparation of melt pool above the fuel support piece inlet, rather than keeping fixed inflow mass rate of 5(kg/s).

It can be seen from the temperature distributions in **Fig 2**, that particle size had large influence on the amount of heat transferred from the melt to the fuel support piece. In the current MPS method, as described in Section 2.2, heat transfer from the melt particle to the adjacent solid particle is calculated based on the temperature difference of the neighboring particles with assumption that heat flux into the midpoint from the hot particle is equal to that out of the midpoint to the cold particle. In fact, temperature and viscosity change of the melt may be large near the wall and the flow is expected to be highly turbulent. These factors are not captured in the current model. Though modeling of the temperature gradient and viscosity gradient may be improved by reducing the particle size, modeling of turbulence may require other techniques such as Large Eddy Simulation [19]. In this paper, influence of the particle size is investigated while consideration of turbulence model may be for future studies.

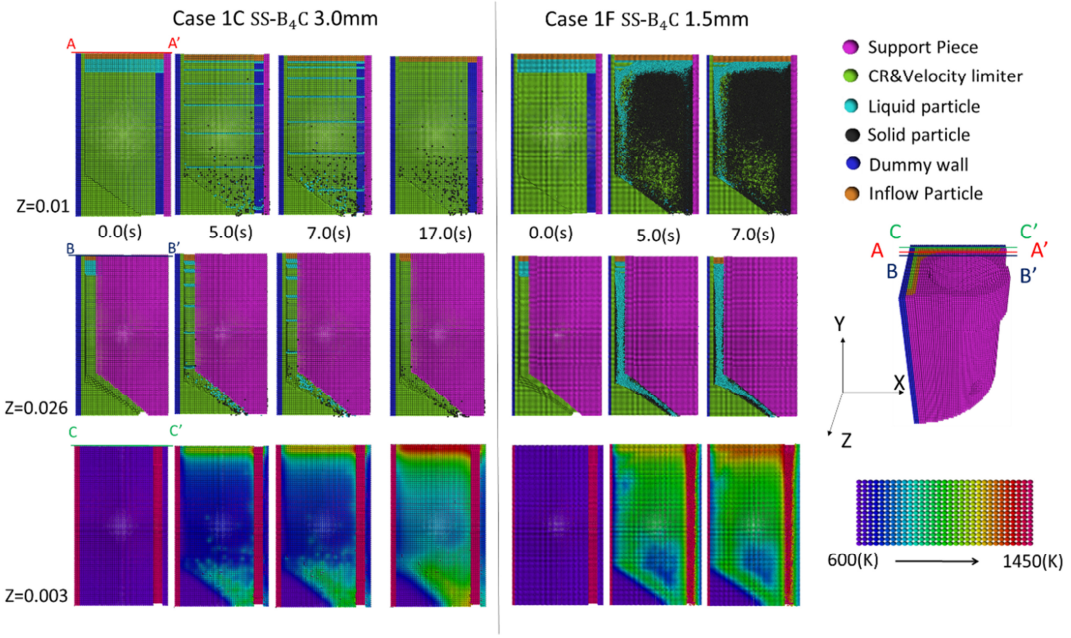

Fig 2. Representative moments depicting the simulated progression of cases 1C and 1F (influence of particle size).

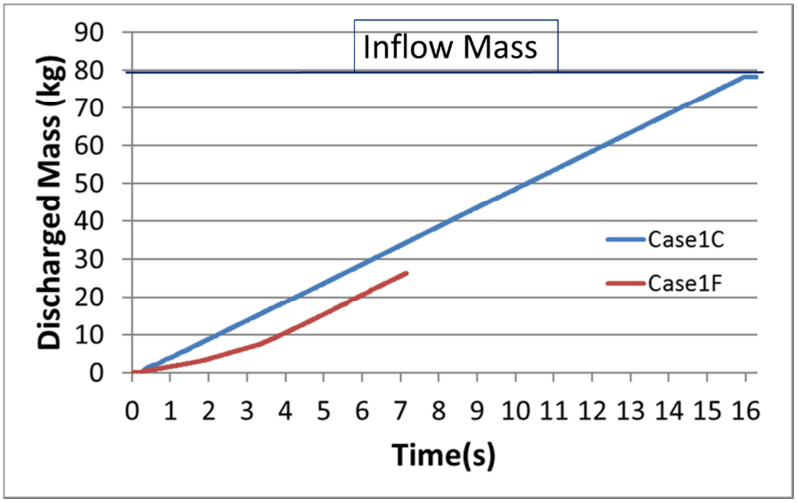

Fig 3. Discharged mass of SS-B_4C eutectic

4.2 Simulations with Zr melt

Figure 4 shows the discharged mass from the bottom of the fuel support piece for the different cases summarized in **Tab 2**. In case 2, complete channel blockages were formed regardless of the particle size, indicating that Zr melt is more likely to form channel blockage than SS-B_4C eutectic under similar initial inflow conditions (inflow mass rate and superheat). This difference may be qualitatively understood from the larger temperature difference between Zr and the fuel support piece, leading to larger heat transfer as well as the smaller latent heat of Zr compared with SS-B_4C eutectic.

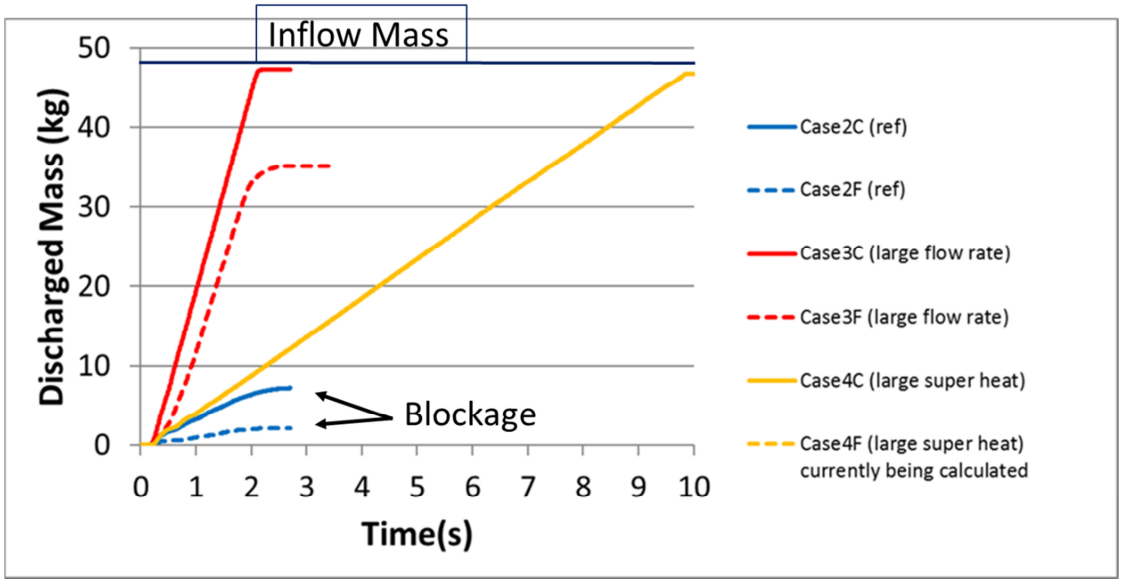

Fig 4. Discharged mass of Zr

Figure 5 shows a series of representative moments for cases 2C and 3C to show influence of the melt inflow rate with coarse calculation resolution (particle size of 3.0 (mm)). In case 2C, solidified particles started to accumulate on the velocity limiter and by approximately 2.5(s),

complete blockage was formed. On the other hand, in case 3C, with larger inflow mass rate, almost all melt particles were discharged with limited blockage. Similarly, **Fig. 6** shows a series of representative moments for cases 2F and 3F to show influence of the melt inflow rate with fine calculation resolution (particle size of 1.5 (mm)). With smaller particle size, the overall formations of blockages were more evident as described in Section 4.1. In case 3F, with larger melt flow rate, the channels by the side and edge of the control rod blade was completely blocked. However, in spite of significant solidification, the pathway above the velocity limiter was not completely blocked, and melt kept being discharged by the end of the simulation.

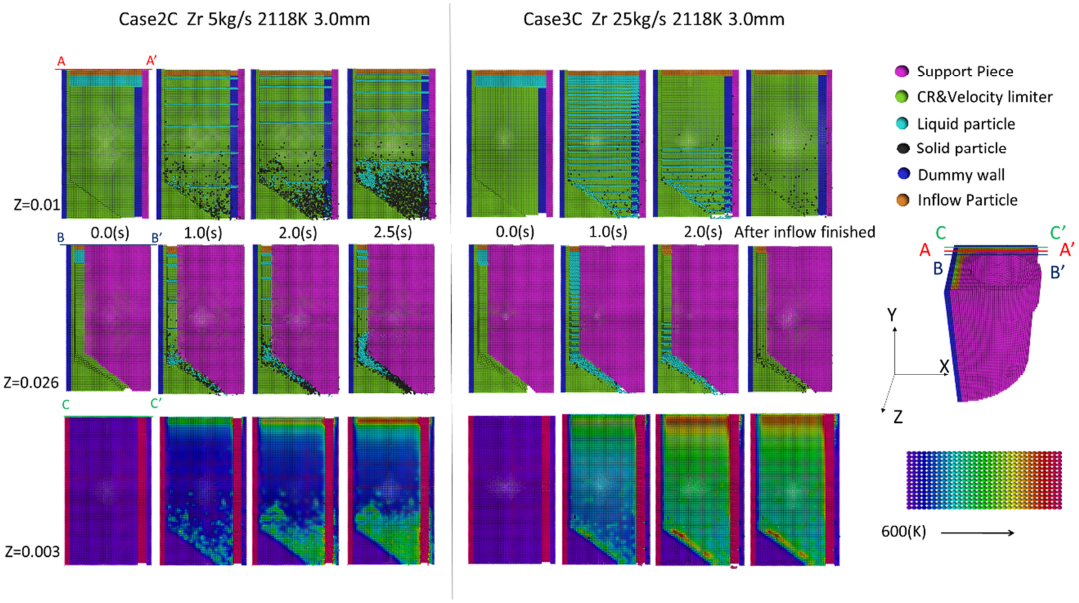

Fig 5. Representative moments depicting the simulated progression of cases 2C and 3C (influence of inflow rate with coarse resolution).

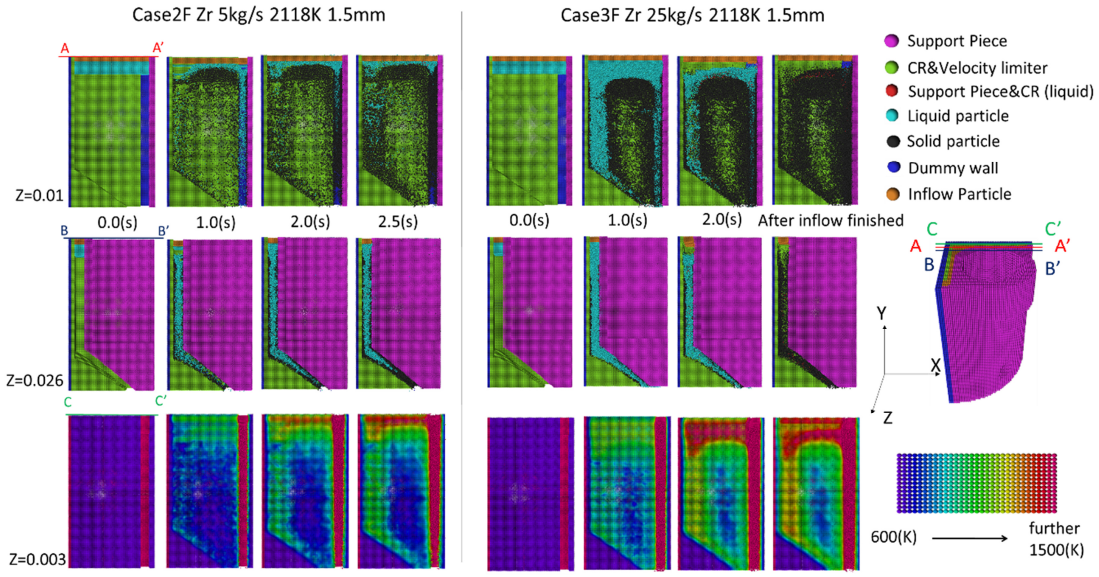

Fig 6. Representative moments depicting the simulated progression of cases 2F and 3F (influence of inflow rate with fine resolution).

In case 4C, the initial melt superheat was increased to 200(K) from 20(K) of the other cases. As the result, blockage didn't occur and solidified particles considerably decreased. However, it should be noted that as shown in Section 4.1, influence of the particle size and possible contributions of turbulence may have to be considered, which should increase effective heat transfer from the melt to the fuel support piece.

5. Conclusion

In this study, metallic Zr and SS-B_4C eutectic melt behaviors through a control rod guide tube of BWR were analyzed by MPS method under dry core degradation condition. The simulation results indicated that channel blockage would form from the side of control rod, and above the velocity limiter. Less blockage was formed near the center of the control rod guide tube. However, the constant melt inflow boundary condition may have influenced formation of the blockage and the inflow boundary condition may have to be revised. The MPS simulations also showed influence of the melt properties (latent heat), initial temperature, and inflow mass rate on the melt behavior qualitatively. However, use of different particle sizes showed significant difference in the heat transfer from the melt to the fuel support piece and the control rod. The current MPS method may need further improvement for analyzing relatively fast heat transfer in a short time, such as use of appropriate particle size and modeling turbulence.

6. References

[1] Tokyo Electric Power Company, "Evaluation of the situation of cores and containment vessels of Fukushima Daiichi Nuclear Power Station Units-1 to 3 and examination into unsolved issues in the accident progression progress report No. 4," Tokyo Electric Power

Company (2015).
[2] OECD NEA “Benchmark Study of the Accident at the Fukushima Daiichi Nuclear Power Plant (BSAF Project) Phase 1 Summary Report,” NEA/CSNI (2015)18.
[3] R.Wachowiak, “Modular Accident Analysis Program (MAAP)-MELCOR Crosswalk Phase 1 Study” Technical Update, November 2014.
[4] B.R. Sehgal *et al.*, “Nuclear Safety in Light Water Reactors, Severe Accident Phenomenology,” ISBN: 978-0-12-388446-6, Elsevier (2012).
[5] M. Naitoh*, M. Pellegrini, A. Takahashi *et al*., “The Findings Obtained During the OECD/NEA BSAF Activity with the Employment of the SAMPSON Code,” NURETH-16, Chicago, IL, August 30-September 4, 2015.
[6] R.O.Gauntt, L.L.Humphries, “Final Results of the XR2-1 BWR Metallic Melt Relocation Experiment”, August 1997.
[7] S. Hagen, P. Hofmann, V. Noack et al., “Dry Core BWR Test CORA-33: Test Results,” KfK 5261, December 1994.
[8] Sandia National Laboratories, ”MELCOR computer code manuals Vol.1: Reference Manual, version2.1”, SAND2015-6692 (2015).
[9] K. Ross, J. Phillips, R.O. Gauntt et al., ”MELCOR Best Practices as Applied in the State-of-the-Art Reactor Consequence Analyses,”, NUREG/CR-7008 (2014).
[10] S.Koshizuka, Y.Oka, “Moving-Particle semi-implicit method for fragmentation of incompressible fluid.”, Nucl. Sci. Eng 123, 421-434(1996).
[11] R.J. Hammersley and R.E. Henry, “Experiments to address lower plenum response under severe accident conditions,” vols. 1 and 2. Electric Power Research Report, EPRI TR-103389 (1994).
[12] R. Chen, Y. Oka, “Numerical analysis of freezing controlled penetration behavior of the molten core debris in an instrument tube with MPS,” Annals of Nuclear Energy 71 (2014) 322-332.
[13] T.Matsuura, Y. Oka, “MPS simulation of spreading behavior of molten materials.” the III International Conference on Particle-based Methods-Fundamentals and Applications Particles, Stuttgart., 2013
[14] T. Kawahara and Y. Oka, “Ex-vessel molten core solidification behavior by moving particle semi-implicit method,” Journal of Nuclear Science and Technology 49, 1156–1164 (2012).
[15] X.Li, A.Yamaji, “A numerical study of isotropic and anisotropic ablation in MCCI by MPS method.”, Progress in Nuclear Energy 90, 46-57. 2016
[16] M.Ramacciotti, C.Journeau, F.Sudreau, G.Cognet, “vicosity models for corium melts. “ Nuclear Engineering and Design 204, 377–389., 2013
[17] T.Sevon, “Status Report of MELCOR Modeling of Fukushima Daiichi 1 Accident”, VTT-R-00215-13, 2013
[18] F.Tanabe, “Analysis of Core Melt Accident in Fukushima Daiichi-Unit 1 Nuclear Reactor”, Nuclear science and technology, Vol.48, No. 8, p.1135-1139(2011)

[19] J.Arai, S.Koshizuka, “Basic Study on Solving Turbulent Flows with Moving Particle Semi-implicit Method”, The Japan Society of Mechanical Engineers, 2007